Progress in Diamond MOSFET Technologies

N. TOKUDA[1], T. MATSUMOTO[1], X. ZHANG[1†], K. SATO[1], K. KOBAYASHI[1], K. ICHIKAWA[1],
K. HAYASHI[1], T. INOKUMA[1], S. YAMASAKI[1], C.E. NEBEL[1,2], M. OGURA[3], H. KATO[3],
T. MAKINO[3], D. TAKEUCHI[3]

[1]Kanazawa University Kakuma-machi, Kanazawa 920-1192, Japan
Phone: +81-76-234-4875 E-mail: tokuda@ec.t.kanazawa-u.ac.jp
[2]Diamond and Carbon Applications, Bürgerwehrstrasse 1, Freiburg 79102, Germany
[3]National Institute of Advanced Industrial Science and Technology, 1-1-1, Umezono, Tsukuba 305-8568, Japan
[†]Present address: North China University of Technology, Shijingshan District, Beijing 100144, China

Keywords: power device, MOS interface, doping, surface control, ultrawide bandgap semiconductor

Abstract

We reported the first inversion channel diamond MOSFETs with normally-off operation and high on/off ratios of over 10^{10} in 2016 [1]. Here, the key technologies were an atomic level control of the epitaxial diamond growth, impurity doping, and the diamond MOS interface. However, the field-effect mobility μ_{FE} of the p-channel diamond MOSFET was 8 cm^2/V·s at the highest, which is much lower than the RT drift and Hall effect hole mobility of 6,300 and 2,200 cm^2/V·s, respectively [2,3]. In this study, we investigated the interface state density D_{it} dependence of μ_{FE} in inversion channel diamond MOSFETs[4]. The interface state could generate around the step edges on diamond surface [5,6]. Recently, we reported selectively buried growth of heavily B doped diamond layers in diamond (111) with atomically step-free surfaces [7]. In this presentation, we will introduce current status and future perspectives on diamond MOSFET technologies.

INTRODUCTION

Carbon is a member of group IV with the least atomic number above Si. Diamond, of which crystal structure is same with that of silicon, has been expected to be the semiconductor material of the next-generation high-power and high-frequency devices because of the superior physical and electronic properties such as extremely high thermal conductivity (20 W/cm·K), carrier mobility (7,300 and 6,300 cm2/V·s for electron and hole, respectively [2]), and breakdown field (10 MV/cm). Actually, there have been many reports about semiconductor devices using diamond for applications like power devices [8-11]. Here, the inversion channel MOSFET is the most important device, because it shows normally-off characteristics. Si, SiC MOSFETs and Si IGBTs based on the MOS structure are widely used because they allow to control the electric power accurately with high tolerance. Recently, we reported the first inversion channel diamond MOSFET with normally-off property and a high on/off ratio of over 10^{10} [1]. However, the field effect mobility and the drain current density were only 8 cm^2/V·s and 1.6 mA/mm, respectively. We attribute the low mobility and the correlated low drain current density to the high interface-state density of 6×10^{12} cm^{-2}·eV^{-1} which is the key factor for carrier scattering. In this study, we investigated the interface-state density (D_{it}) dependence of the carrier mobility (μ_{FE}) in inversion channel diamond MOSFETs.

EXPERIMENTAL

Figure 1(a) shows a schematic image of a cross-sectional structure of the typical inversion channel diamond MOSFET fabricated on HPHT synthetic N-doped semi-insulating single-crystal diamond (111) substrate. Here, L_g and W_g are the gate electrode length and width, respectively. The fabrication process was as follows. Firstly, P-doped diamond films as n-type bodies were grown onto each HPHT diamond (111) substrate by MPCVD. The P concentrations of the n-type bodies (N_P) were 2×10^{15}, 1×10^{16}, 3×10^{16}, and 6×10^{16} cm^{-3}. Second, p$^+$-type layers (B doping) for source/drain formation including hole injection into inversion channel were selectively grown on each n-type body through a metal mask by MPCVD because ion implantation technique into diamond has not been established yet. The thickness and B concentration of the p$^+$-type layers were about 50 nm and about 10^{21} cm^{-3}, respectively. Third, after removing the metal mask by acid cleaning, the samples were treated by water vapor annealing in an electric furnace at 500 °C for 60 min under an atmosphere of N_2 gas bubbled through ultrapure water in a quartz tube to obtain stable OH surface terminations [12]. Al_2O_3 films with 30~50 nm thick were then deposited onto each sample by ALD at 300 °C. When the Al_2O_3 layer was deposited, the termination of the diamond surface changed from OH to O because the chemical reaction between OH and trimethylaluminum is identical to that in the ALD mechanism. The ALD-Al_2O_3 deposition on the OH-termination is a key process for achieving the inversion-channel formation at the diamond MOS interface. Finally, gate, drain, and source electrodes (Ti/Pt/Au) were fabricated on each sample by photolithography and lift-off techniques. L_g and W_g were 15 and 100 μm, respectively.

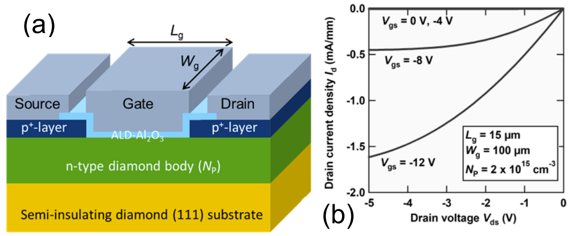

Fig. 1 (a) Schematic image of a cross-sectional structure of an inversion channel diamond MOSFET. (b) I_d–V_{ds} characteristics of the inversion channel diamond MOSFET. Reprinted with permission from Ref. [4] (https://creativecommons.org/licenses/by/4.0/).

RESULTS AND DISCUSSION

Figure 1(b) shows the drain current density (I_d) as a function of drain voltage (V_{ds}) for different gate potentials (V_{gs}) of the inversion channel diamond MOSFET with N_P of 2×10^{15} cm^{-3}, L_g of 15 µm, and W_g of 100 µm measured in air at 300 K [8]. We varied the gate voltage (V_{gs}) between 0 and -12 V with steps of -4 V. The drain source voltage was changed between 0 and -5 V with voltage steps of -0.1 V. Gate leakage current values were 27 pA/mm at $V_g = -9$ V and 110 nA/mm at $V_g = -12$ V. The MOSFET exhibits normally-off properties and clear saturation characteristics. The drain current is well modulated by the gate potential. The maximum I_d was -1.6 mA/mm. The threshold voltage V_T is –0.9 V.

Figure 2 demonstrates the correlation between μ_{FE} and D_{it} for the diamond MOSFETs. Note that the reported D_{it}–μ_{FE} results of other diamond MOSFETs with different surface terminations are also inserted [10,11,13]. We can see that the μ_{FE} and D_{it} are inversely correlated. Thus, the high D_{it} is one main limiting factor for the channel mobility of diamond MOSFETs. From the changing tendency of D_{it}–μ_{FE} demonstrated by the arrow inserted in Fig. 2, we can expect that μ_{FE} can exceed 1000 $cm^2V^{-1}s^{-1}$ if D_{it} is reduced to lower than 10^{11} $cm^{-2}eV^{-1}$[14]. This is consistent with the theoretical mobility calculation by considering four scattering mechanisms for the diamond MOSFET by Daligou and Pernot *et al.* [15]. They suggest that demonstrates that a high hole mobility up to 3000 cm^2/Vs can be achieved in p-ch diamond FETs with the use of an atomically flat interface and trap density lower than 10^{10} cm^{-2}. Therefore, it is very important to develop effective passivation processes to reduce D_{it} and improve the interface quality between Al_2O_3 and diamond and thus fabricate the diamond power MOSFETs with superior electrical properties.

CONCLUSIONS

We successfully fabricated inversion channel diamond MOSFETs with normally-off characteristics and high on/off ratios using a high-quality insulated phosphorus doped n-type diamond body. The data reveal that the mobility of the inversion channel diamond MOSFETs are significantly affected by the (high) interface state densities and indicate the key problem for the realization of high-power and high-frequency diamond devices.

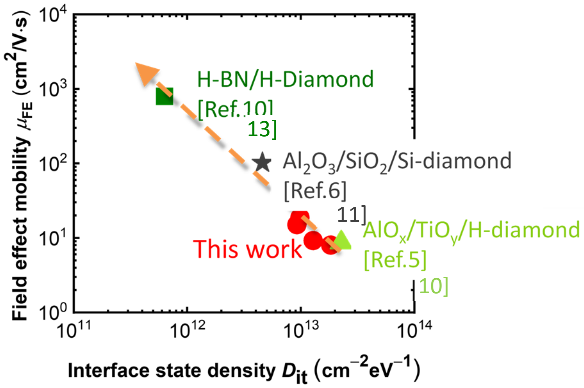

Fig. 2. The correlation between D_{it} and μ_{FE} of the diamond MOSFETs. Reprinted with permission from Ref. [14] (https://creativecommons.org/licenses/by/4.0/).

Acknowledgements

This work was partially supported by MEXT-Program for Creation of Innovative Core Technology for Power Electronics Grant Number JPJ009777, Kanazawa University CHOZEN Project 2022, a NEDO Feasibility Study Program (Uncharted Territory Challenge 2050) grant number 19101600-0, JST FOREST Program (Grant Number JPMJFR20353078, Japan), and JSPS KAKENHI grant numbers JP18KK0383 and JP21H01363.

REFERENCES

[1] T. Matsumoto, NT *et al.*, Sci. Rep. **6**, 31585 (2016).
[2] I. Akimoto, N. Naka, NT, Diamond Relat. Mater. **63**, 38 (2016).
[3] V.S. Bormashov *et al.*, Diamond Relat. Mater. **35**, 19 (2013).
[4] T. Matsumoto, NT *et al.*, Appl. Phys. Lett. **114** , 242101 (2019).
[5] M. Nagai, NT *et al.*, Jpn. J. Appl. Phys. **58**, SIIB08 (2019).
[6] Y. Ogata, NT *et al.*, Mater. Sci. Forum **1062**, 298 (2022).
[7] K. Kobayashi, NT *et al.*, Appl. Surf. Sci. **593**, 153340 (2022).
[8] M. Suzuki *et al.*, Phys. Status Solidi A **210**, 2035 (2013).
[9] D. Takeuchi *et al.*, Jpn. J. Appl. Phys. **51**, 090113 (2012).
[10] J. Liu *et al.*, Carbon **172**, 112 (2021).
[11] W. Fei *et al.*, Appl. Phys. Lett. **116**, 212103 (2020).
[12] R. Yoshida, NT *et al.*, Appl. Surf. Sci. **458**, 222 (2018).
[13] Y. Sasama *et al.*, Nat. Electron. **5**, 37 (2022).
[14] X. Zhang, NT *et al.*, J. Mater. Res., **36**, 4688 (2021).
[15] G. Daligou, J. Pernot, Appl. Phys. Lett., **116**, 162105 (2020).

ACRONYMS

IGBT: Insulated-Gate Bipolar Transistor
HPHT: High-Pressure High-Temperature
MPCVD: Microwave Plasma-assisted Chemical Vapor Deposition
ALD: Atomic Layer Deposition